Journal of Peptide Science
J. Peptide Sci. 2006; **12**: 82–91
Published online 20 December 2005 in Wiley InterScience (www.interscience.wiley.com). DOI: 10.1002/psc.743

JOURNAL OF PEPTIDE SCIENCE

Conformational analysis of a potent SSTR3-selective somatostatin analogue by NMR in water solution

MARGARIDA GAIRÍ,[a] PILAR SAIZ,[b] SERGIO MADURGA,[b] XAVIER ROIG,[b] JUDIT ERCHEGYI,[c] STEVEN C. KOERBER,[c] JEAN CLAUDE REUBI,[d] JEAN E. RIVIER[c] and ERNEST GIRALT[b,e]*

[a] NMR Facility, Serveis Cientificotècnics, University of Barcelona, Barcelona Science Park, Josep Samitier 1-5, 08028 Barcelona, Spain
[b] Biomedical Research Institute, Barcelona Science Park, Josep Samitier 1-5, 08028 Barcelona, Spain
[c] The Clayton Foundation Laboratories for Peptide Biology, The Salk Institute for Biological Studies, 10010 North Torrey Pines Road, La Jolla, California 92037, USA
[d] Division of Cell Biology and Experimental Cancer Research, Institute of Pathology, University of Berne, Berne, Switzerland
[e] Department of Organic Chemistry, University of Barcelona, Martí i Franquès 1-11, 08028 Barcelona, Spain

Received 4 November 2005; *Revised 6 November 2005*; *Accepted 10 November 2005*

Abstract: The three-dimensional structure of a potent SSTR3-selective analogue of somatostatin, cyclo(3–14)H-Cys^3-Phe^6-Tyr^7-D-Agl^8(N$^\beta$ Me, 2-naphthoyl)-Lys^9-Thr^{10}-Phe^{11}-Cys^{14}-OH (des-AA^{1,2,4,5,12,13}[Tyr^7, D-Agl^8(N$^\beta$ Me, 2-naphthoyl)]-SRIF) (peptide **1**) has been determined by ^{1}H NMR in water and molecular dynamics (MD) simulations. The peptide exists in two conformational isomers differing mainly by the *cis*/*trans* isomerization of the side chain in residue 8. The structure of **1** is compared with the consensus structural motifs of other somatostatin analogues that bind predominantly to SSTR1, SSTR2/SSTR5 and SSTR4 receptors, and to the 3D structure of a non-selective SRIF analogue, cyclo(3–14)H-Cys^3-Phe^6-Tyr^7-D-2Nal^8-Lys^9-Thr^{10}-Phe^{11}-Cys^{14}-OH (des-AA^{1,2,4,5,12,13}[Tyr^7, D-2Nal^8]-SRIF) (peptide **2**). The structural determinant factors that could explain selectivity of peptide **1** for SSTR3 receptors are discussed. Copyright © 2005 European Peptide Society and John Wiley & Sons, Ltd.

Keywords: somatostatin analogues; NMR; betidamino acid; *cis–trans* conformational isomers; molecular dynamics; SSTR3 selectivity; pharmacophore

INTRODUCTION

It is well known that peptides play a major role in signalling processes in the central nervous system. Frequently, the same molecule is able to interact with many different receptors carrying out several biological functions. One of the most paradigmatic cases illustrating this behaviour is that of somatostatin or somatotropin release inhibiting factor (SRIF), H-Ala^1-Gly^2-c[Cys^3-Lys^4-Asn^5-Phe^6-Phe^7-Trp^8-Lys^9-Thr^{10}-Phe^{11}-Thr^{12}-Ser^{13}-Cys^{14}]-OH [1], a cyclic tetradecapeptide that acts as a neurotransmitter and neuromodulator in the central nervous system [2], as an inhibitor of the release of numerous hormones [3] and as a regulator of cell proliferation and differentiation [4]. SRIF is able to establish high-affinity interactions with a family of at least five different receptor subtypes, somatostatin receptor (SSTR) 1–5 [4,5]. Despite the fact that all receptors share common signalling pathways, they have specific functional roles, and some biological responses show subtype selectivity. For example, SSTR2 principally mediates the inhibition of the release of glucagon and growth hormone [6]. SSTR5 controls insulin secretion, and both SSTR2 and SSTR5 mediate the antiproliferative effects of somatostatin on cellular growth processes in tumours [7,8]. However, the individual functions of the different somatostatin receptors *in vivo* are still not fully understood.

Because of its wide range of physiological functions, SRIF is a target for development of receptor subtype-specific analogues. Nowadays, hundreds of somatostatin analogues [9] are available, which bind with some selectivity to receptor subtypes and extensive structural studies have been done to ascertain the minimum structural requirements of the analogues for selective binding. So far, a different pharmacophore model has been proposed for analogues binding predominantly to SSTR1 [10], SSTR2/SSTR5 [11,12] and SSTR4 [13] receptors. It seems that the consensus structural motif for any of these selective ligands requires a unique arrangement of several side chains, which are important for selective binding. For SSTR3-selective analogues, no structural information is available so far to understand their binding affinity and selectivity. Some years ago, Reubi *et al.* [14] reported a group of potent SSTR3-selective analogues containing betidamino acids (*N*′-monoacylated aminoglycine

Abbreviations: Agl, aminoglycine; AGL^8, D-Agl^8(N$^\beta$ Me, 2-naphthoyl); Ar, aromatic residue; CNS, Crystallography and NMR system; DQF-COSY, double-quantum-filtered correlated spectroscopy; MD, Molecular Dynamics; NMR, Nuclear Magnetic Resonance; NOE, Nuclear Overhauser Effect; NOESY, Nuclear Overhauser Spectroscopy; 2-Nal, 2-naphthylalanine; ROESY, Rotating-frame Overhauser Enhancement Spectroscopy; SRIF, Somatostatin or Somatotropin Release Inhibiting Factor; SSTR, somatostatin receptor; TOCSY, Total Correlation Spectroscopy.

*Correspondence to: E. Giralt, Institut de Recerca Biomèdica, Parc Científic de Barcelona-Universitat de Barcelona, Josep Samitier 1-5, 08028-Barcelona, Spain; e-mail: egiralt@pcb.ub.es

derivatives in which the *N′*-acyl/alkyl group may mimic naturally occurring amino acid side chains or introduce novel functionalities) [15], which are competitive antagonists. In this paper, we present the conformational study by nuclear magnetic resonance (NMR) of one of these analogues: des-AA^{1,2,4,5,12,13}-[Tyr^7, D-Agl^8(N$^{\beta}$ Me, 2-naphthoyl)]-SRIF (peptide **1** in this paper), a potent and SSTR3-selective antagonist ($IC_{50} = 70 \pm 18$ nM), which does not bind to receptors SSTR1, SSTR2, SSTR5 ($IC_{50} > 10\,000$ nM) or SSTR4 ($IC_{50} > 1000$ nM).

NMR is the most useful tool to carry out conformational studies of peptidic molecules in solution. Unfortunately, most peptides are so flexible in aqueous media that scarce structural information can be obtained by standard techniques. The usual way to circumvent the problem is to work in more apolar environments, usually in organic solvents (Grace, C. R. R., Erchegyi, J., Reubi, J. C., Rivier, J., Riek, R., in preparation). In our experience, however, when the target is an elaborate and highly selective compound, it is often structured enough to be studied in aqueous media. This is the case with peptide **1**. In this paper, we present the 3D structure determination of this somatostatin analogue in water, we discuss the possible reasons for its SSTR3-selectivity and we compare the 3D structure with that of another somatostatin analogue: des-AA^{1,2,4,5,12,13}-[Tyr^7, D-2Nal^8]-SRIF (peptide **2**) which, despite the high similarity to peptide **1**, is an agonist and has totally lost selectivity for SSTR3 receptors ($IC_{50} > 1000$ nM at SSTR1; 57 nM at SSTR2; 3.4 nM at SSTR3; 1.4 nM at SSTR4 and 13 nM at SSTR5) [16]

MATERIALS AND METHODS

Sample Preparation and NMR Experiments

Analogues were synthesized, as described in [14]. NMR samples were prepared by dissolving about 3 mg of the analogue in 0.7 ml of a 0.01 mM NaN_3 solution containing 15% D_2O in H_2O. The ^{1}H NMR spectra were recorded on a Bruker 800-MHz spectrometer (peptide **1**) and a Bruker 600-MHz instrument (peptide **2**). Dioxane was used as internal standard ($\delta = 3.75$ ppm). A series of 1D spectra were acquired at different temperatures: 278 K, 283 K, 288 K, 293 K, 298 K and 303 K in order to measure the temperature coefficients of the amide protons. All 2D spectra were measured at 278 K. ^{1}H resonances assignment was carried out using the standard sequential assignment protocol developed by Wüthrich [17], based on 2D total correlation spectroscopy (TOCSY) [18], double-quantum-filtered correlated spectroscopy (DQF-COSY) [19] experiments for intraresidual assignment and 2D nuclear overhauser spectroscopy (NOESY) [20] and rotating-frame overhauser enhancement spectroscopy (ROESY) [21] experiments for sequential assignment. The TOCSY experiments employed the DIPSI-2 spin-locking sequence applied for a mixing time of 80 ms. The NOESY experiments were carried out with mixing times of 200 ms and 400 ms, and the ROESY with a mixing time of 200 ms. The TOCSY, NOESY and DQF-COSY experiments were acquired with 64, 64–72 and 64 scans respectively, and a relaxation delay of 1.4–1.5 s. The TOCSY, NOESY and ROESY spectra were carried out using 2048×512 (real data points) and zero filled to 2048×1024 before Fourier transformation. The DQF-COSY spectra were acquired with 2048×950 (real data points) and were zero filled to 2048×2048 before Fourier transformation. Water suppression was carried out with the Watergate sequence [22] in the TOCSY, NOESY and ROESY experiments and with an excitation sculpting [23] scheme in the DQF-COSY experiments. Stereospecific assignments for β-methylene protons (Table 1) have been achieved by analysing the cross-peak J-coupling patterns in *E*-COSY experiments [24] and the intra-residue nuclear overhauser effect (NOEs) between NH, αH and βH protons [25]. All of the spectra were processed, both using the XWINNMR program from Bruker and the NMRPipe [26] program and analysed using both the XWINNMR and the NMRView [27] programs.

Structure Calculation

Distance restraints for structure calculations were derived from cross-peaks in NOESY spectra recorded at 278 K (solvent: 15% D_2O/H_2O) with a mixing time of 400 ms. The cross-peak intensities were estimated from contour levels and were classified according to their intensities and grouped into four categories corresponding to upper-bound inter-proton distance restraints of 2.8, 3.4, 5 and 6 Å, respectively. Appropriate pseudo atoms corrections were applied to non-stereospecifically assigned protons. Torsion angle restraints (Φ) derived from $^3J_{NH\alpha H}$ coupling constants were incorporated according to the following: $-120^\circ \pm 40^\circ$ for $^3J_{NH\alpha H} > 9$ Hz and: $-120^\circ \pm 50^\circ$ for $^3J_{NH\alpha H} > 8$ Hz.

The computational protocol for structural determination of each peptide (conformational isomers *Z* and *E* of peptide **1** and peptide **2**) consisted of restrained molecular dynamics (MD) simulation employing the crystallography and NMR system (CNS) program [28], version 1.1 (http://cns.csb.yale.edu/v1.1/) with the CHARMM19 force field. Parameters and topology of the non-natural amino acids were found at the Gerard Kleywegt's HIC-Up database [29] and added to the corresponding CNS libraries, protein-allhdg.top and protein-allhdg.param. The standard Simulated Annealing protocol implemented in the CNS program was used. MD in torsion-angle space was applied to structure calculation starting from an extended conformation. In the first stage, the regularized extended strands were submitted to 15 ps of torsion-angle MD at 50 000 K. The scale factor for the van der Waals energy term was set to 0.1 to facilitate rotational barrier crossings. The structures were then subjected to a slow-cooling torsion-angle MD stage in which the temperature was reduced from 50 000 to 2000 K over a period of 15 ps, while the van der Waals scale factor was linearly increased from 0.1 to 1.0. Afterwards, the temperature was decreased to 300 K during another slow cooling stage over 6 ps. A total of 50 structures were calculated for each peptide. Finally, each resultant structure was subjected to 2000 steps of conjugate-gradient minimization. The best ten conformers were selected on the basis of the total energy and residual violations. Conformers with the lowest overall energies only, and having no violations of distance restraints >0.5 Å and no violations of dihedral

Table 1 Proton Chemical Shifts (ppm) of Peptides **1** and **2**

Residue		**1** major	**1** minor	**2**
Cys^3	αH	4.28	4.34	4.24
	βH	3.14^S, 2.85^R	3.31^S, 2.90^R	3.25, 2.99
Phe^6	NH	8.48	8.98	9.02
	αH	4.53	4.62	4.73
	βH	2.91	3.15, 3.02	2.97
	H2,6	6.95	7.37–7.34	6.97
	H3,5	6.70	7.44–7.41	7.17
	H4	6.86	—	—
Tyr^7	NH	8.74	8.69	8.28
	αH	4.16	4.39	4.42
	βH	3.10^R, 2.73^S	3.15^R, 2.75^S	2.93, 2.82
	H2,6	7.14	7.14	7.08
	H3,5	6.90	6.80	6.82
D-2Nal^8/ AGL^8		AGL^8	AGL^8	D-2Nal^8
	NH	9.34	8.95	8.48
	αH	6.09	6.25	4.52
	βH	—	—	3.04, 2.89
	H1	7.87	7.92	7.59
	H3	7.47	7.40	7.28
	H4	8.11	8.05	7.88
	H5	8.08–8.00	8.08–8.00	7.87
	H6	7.7–7.6	7.7–7.6	7.55
	H7	7.7–7.6	7.7–7.6	7.53
	H8	8.08–8.00	8.08–8.00	7.92
	N-CH_3	2.38	2.62	—
Lys^9	NH	7.81	8.28	8.45
	αH	4.49	4.56	4.16
	βH	1.71, 1.47	1.89, 1.87	1.56, 1.28
	γH	1.20, 1.12	1.52, 1.44	0.48, 0.25
	δH	1.57, 1.51	1.71, 1.68	1.06
	εH	2.80	2.98	2.18
	NH_3^+	7.61	7.62	7.36
Thr^{10}	NH	8.55	8.52	8.00
	αH	4.08	4.11	4.26
	βH	4.08	4.08	4.06
	γH	0.99	0.98	1.09
Phe^{11}	NH	7.86	7.88	8.33
	αH	4.75	4.78	4.69
	βH	3.18, 3.02	3.19, 3.03	3.24, 3.06
	H2,6	7.26–7.23	7.26–7.23	7.36
	H3,5	7.36–7.31	7.31–7.27	7.28
	H4	—	—	—
Cys^{14}	NH	8.43	8.49	8.23
	αH	4.55	4.60	4.54
	βH	3.10	3.22, 3.17	3.17

Stereospecifical assignment of βH protons has only been possible for Cys^3 and Tyr^7 of peptide **1**. Prochiral atoms are labelled R and S to indicate proR and proS according to the Cahn–Ingold Prelog rules.

angle restraints >5°, were retained for analysis. Structures were analysed and visualized using the VMD-XPLOR [30] and PyMol [31] programs.

RESULTS AND DISCUSSION

The chemical shift assignment of proton resonances for peptides **1** and **2** has been carried out using 2D NMR experiments as described in the section on 'Materials and Methods'. The *N*-terminal amino protons for both analogues were not observed due to the fast exchange with the solvent. Peptide **1** showed two conformations in water perfectly distinguishable in the NMR timescale, while peptide **2** presented only one conformation in aqueous solution.

The 1D ^{1}H NMR spectrum of peptide **1** in water shows two sets of signals for all of the seven amide protons (Figure 1), whose relative integration indicates the presence of two conformational isomers in a 3 : 2 ratio (major : minor). Most of the ^{1}H resonances of each isomer have been assigned (Table 1). Only the aromatic protons of Phe^{11} and some aromatic protons of the naphthoyl in residue 8 showed a strong overlap between both isomers, which precluded their assignment. The main ^{1}H chemical shift differences between the major and the minor isomers are concentrated in three residues: Phe^6, AGL^8 and Lys^9 and specially involve the NH protons, the aromatic protons of Phe^6 and the side-chain protons of Lys^9.

The existence of peptide **1** as two conformational isomers arises from the *cis–trans* isomerization of the amide bond present in the side chain of the betidamino acid 8. The process is slow enough in the NMR timescale to allow the observation of each isomer independently. Intra-residue NOEs involving the side-chain protons of this betidamino acid constitute the first evidence of the *cis–trans* isomerization. The observation of medium H1/N-CH_3 and H3/N-CH_3 NOEs (present both in NOESY and ROESY spectra) in the minor isomer is a clear diagnostic of the ***E*** isomer (*trans* orientation of the naphthyl group and the Cα), as can be seen in Figure 2. Moreover, the presence of a strong HN/N-CH_3 NOE, and medium αH/N-CH_3, H1/αH, H3/αH NOEs in the major isomer is clear evidence of the ***Z*** isomer (*cis* orientation of the naphthyl and the Cα). As will be discussed later, the result of calculating the solution 3D structure independently for each isomer of peptide **1** confirms that the major conformer corresponds to the ***Z*** isomer and the minor conformer to the ***E*** isomer.

Following the protocol described in the section on 'Materials and Methods', distance and dihedral angle restraints were used as input for the structure calculation with the program CNS. For both the major and the minor conformational isomers, the ten conformations having the lowest energies and small residual restraint violations (Table 2) were analysed considering they represent the 3D solution structure of the major and the minor isomers of peptide **1**, respectively. The torsion angles (Φ, Ψ, χ_1) of the bundle of these ten conformers are listed in Table 3.

The 3D structure of the major isomer shows a turn around the Tyr^7 and AGL^8 residues. However,

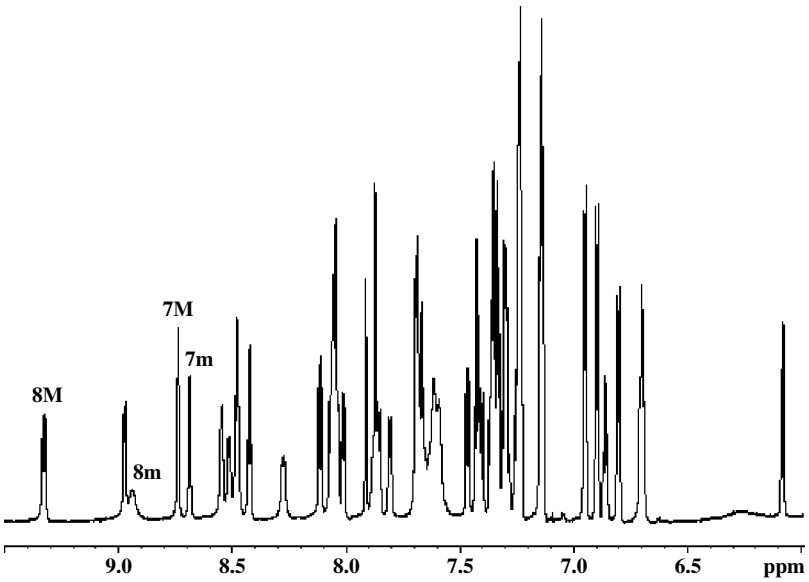

Figure 1 Low-field region of the 1D ^{1}H spectrum of peptide **1**. The amide proton signals of Tyr^7 (**7M/7m**) and AGL^8 (**8M/8m**) are labelled to illustrate the presence of two conformational isomers. **M** refers to the major isomer and **m** to the minor one.

Table 2 Characterization of the ensemble of ten conformers representing the NMR structures of peptides **1** and **2**

Peptide	NOE distance restraints	Φ angle restraints	Backbone rmsd[a] (Å)	All atoms rmsd (Å)	CHARMM19 energies (kcal/mol)		NMR derived restraints violations			
					Total energy	v. der Waals	Distances viol. >0.5 Å		Dihedral angles viol. >5°	
							no.	rmsd (Å)	no.	rmsd (°)
1 major	48	4	0.69 ± 0.32	1.56 ± 0.35	22.2 ± 1.2	7.0 ± 0.3	0	0.004 ± 0.003	0	0.137 ± 0.046
1 minor	40	4	0.80 ± 0.22	1.87 ± 0.52	22.7 ± 1.1	7.3 ± 0.4	0	0.009 ± 0.003	0	0.010 ± 0.019
2	52	3	1.03 ± 0.26	2.13 ± 0.24	23.9 ± 1.1	6.7 ± 0.4	0	0.009 ± 0.004	0	0.019 ± 0.039

[a] Average and standard deviation of the rmsd from the mean structure for backbone atoms (O, C, C$^\alpha$, N).

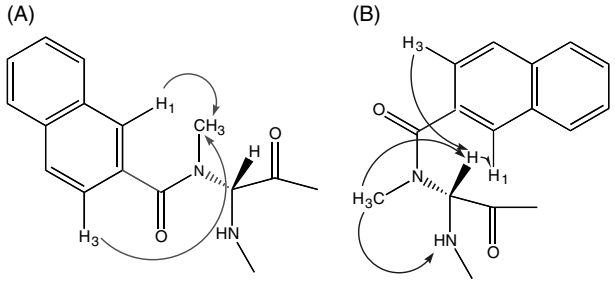

Figure 2 Intra-residue NOEs observed between side-chain protons of AGL^8 for the minor, ***E*** (A) and the major, ***Z*** (B) conformational isomers of peptide **1**.

on the basis of the backbone torsion angles, it does not exhibit any type of canonical β-turn [32], despite the pattern of sequential and medium-range backbone NOEs (Figure 3(A)) involving the Phe^6-Tyr^7-AGL^8-Lys^9 residues. Although the temperature coefficient of the amide proton of Lys^9 is relatively high (−5.2 ppb/K), close to typical values for solvent exposed amide protons (−6/−8.5 ppb/K) [33], the carbonyl C=O of Phe^6 is in a hydrogen-bond favourable orientation and the distance Lys^{9}HN-O′Phe^6 is compatible with the existence of hydrogen bonding. On the other hand, the amide proton of Phe^{11}, with a temperature coefficient of −3.5 ppb/K, does not have an acceptor partner properly orientated and close enough to be involved in hydrogen bonding.

A *cis* amide bond (***Z*** isomer) in the side chain of AGL^8 is present in all of the ten final conformers, supported by the intra-residue NOEs previously mentioned. The side chains of Phe^6, AGL^8 and Lys^9, quite well defined, are close to each other in space and perpendicularly orientated with respect to the backbone plane of the peptide (Figure 4(A)). The side chain of Phe^6 is in the *trans* rotamer and that of Lys^9 is in the *gauche*$^-$ rotamer. The nomenclature recommended in [34] has

Table 3 Torsion angles (in degrees) of the ensemble of ten calculated structures for peptides **1** and **2**

Residue	Peptide **1** major			Peptide **1** minor			Peptide **2**		
	Φ	Ψ	χ^1	Φ	Ψ	χ^1	Φ	Ψ	χ^1
Phe^6	−89 ± 27	143 ± 12	177 ± 1	−95 ± 34	80 ± 130	−83 ± 70	−93 ± 104	109 ± 22	176 ± 4
Tyr^7	−78 ± 12	69 ± 8	130 ± 98	−43 ± 48	114 ± 26	178 ± 2	−133 ± 21	98 ± 26	176 ± 6
D-2Nal^8/AGL^8	−160 ± 0	−38 ± 22	138 ± 5	44 ± 143	−36 ± 24	12 ± 79	69 ± 74	−93 ± 24	128 ± 95
Lys^9	−88 ± 15	95 ± 137	−61 ± 3	−103 ± 25	122 ± 100	−74 ± 35	−155 ± 9	30 ± 45	−2 ± 82
Thr^{10}	−103 ± 10	44 ± 8	48 ± 64	−97 ± 13	−31 ± 17	60 ± 2	−146 ± 15	−165 ± 2	178 ± 1
Phe^{11}	−143 ± 12	148 ± 23	−82 ± 69	−124 ± 19	110 ± 37	−27 ± 54	−64 ± 68	114 ± 99	−1 ± 96

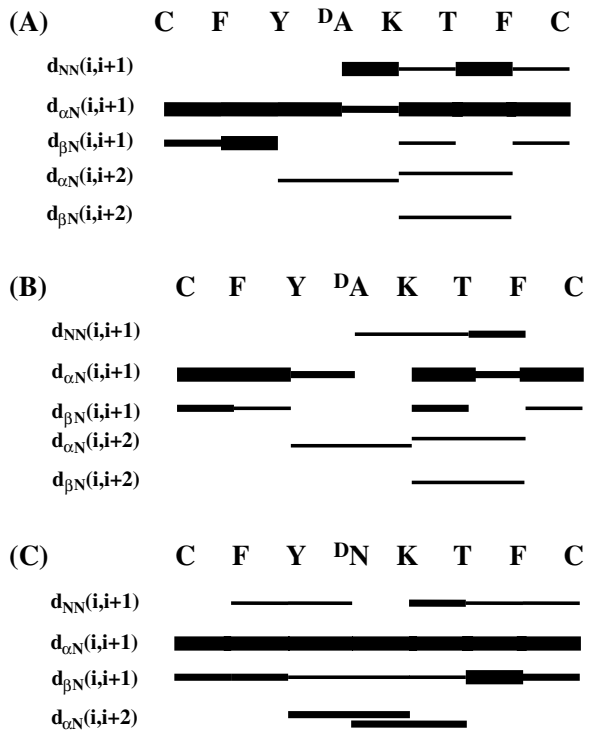

Figure 3 Characteristic sequential and medium-range NOEs used for the structure calculation of peptide **1**: major conformational isomer **(A)** and minor conformational isomer **(B)**; and peptide **2 (C)**. Residues designated with DA and DN correspond to the amino acid AGL^8 and D-2Nal^8, respectively.

been used to describe side-chain torsion angles: *trans* refers to $\chi^1 = 180°$, *gauche*$^+$ refers to $\chi^1 = +60°$ and *gauche*$^-$ refers to $\chi^1 = -60°$. The proximity of these two side chains is confirmed by a few NOEs involving the aromatic protons of Phe^6 and the βH and γH of Lys^9. The Tyr^7 side chain is oriented in the opposite direction with respect to the previous side chains. Phe^{11} is not very well defined and explores a large region of conformational space. Despite the fact that the aromatic ring is close to Lys^9 side chain in some of the calculated conformations, only a βH–βH NOE involving the side chains of these two residues is observed. The absence of NOEs involving the aromatic protons of Phe^{11} and the Lys^9 alkyl protons agrees with the poor definition of the Phe^{11} side chain.

The 3D structure of the minor conformational isomer shows that the backbone is quite similar to that of the major isomer. The backbone torsion angles are not compatible with any type of β-turn, despite the pattern of backbone NOEs (Figure 3(B)). The low temperature coefficient found for the amide proton of Phe^{11} (−1.3 ppb/K) suggests its participation in a hydrogen bond [33]. In the calculated structures, the oxygen in the side chain of Thr^{10} is the only possible hydrogen bond acceptor for the NH of Phe^{11}. On the other hand, side chains adopt different orientations in the major and minor isomers. The amide bond in the side chain of AGL^8 shows a *trans* orientation of the naphthyl and Cα (isomer ***E***) in the ten analysed conformers for the minor isomer supported by the previously mentioned intra-residue NOEs. This *trans* conformation moves the naphthyl ring away from the Phe^6 and Lys^9 side chains and brings it over the aromatic ring of Tyr^7 (Figure 4(B)). Actually, the aromatic rings of Tyr^7 and AGL^8 are quite well defined in all of the ten conformers and remain adjacent and almost parallel to each other in space, adopting an equatorial disposition with respect to the macrocycle of the peptide backbone. The aromatic ring of Phe^6 spans a large region of conformational space and stays far from the previous aromatic residues (Ar). The side chain of Lys^9 orients itself perpendicularly to the backbone plane farther away from the aforementioned side chains. Globally, the 3D structure of the minor conformational isomer is more flat and extended than the structure of the major one.

The differences between the 3D structures of the ***Z*** and ***E*** isomers (Figure 4) are consistent with the experimental proton chemical shift differences observed for some residues. The aromatic ring of Phe^6 and the naphthyl of AGL^8 are well defined in the 3D structure of the major isomer. The relative orientation of these two side chains could favour an aromatic π–π interaction in an edge-face geometry [35]. Chemical shifts of Phe^6 aromatic protons in the major isomer resonate at lower frequencies (upfield shift) than those in the minor

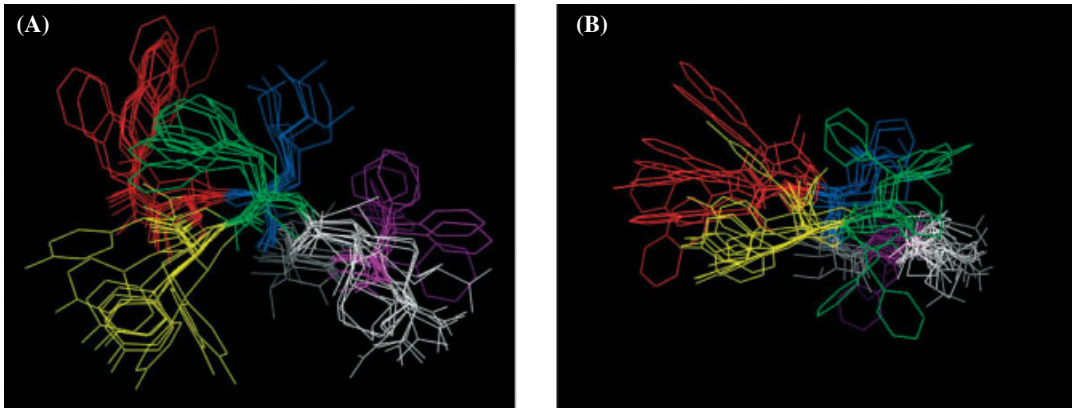

Figure 4 Bundle of ten conformers representing the 3D structures of the major (A) and minor (B) conformational isomers of peptide **1**. The side chains of some residues are coloured: Phe^{6} (green), Tyr^{7} (yellow), AGL^{8} (red), Lys^{9} (blue) and Phe^{11} (magenta).

one (Table 1), reflecting the ring current effect caused by the spatially close naphthyl ring. The Lys^{9} side-chain protons also show an upfield shift in the major isomer, *versus* the minor one, reflecting the proximity of the amino-alkyl chain to the aromatic rings of Phe^{6} and AGL^{8}. In accordance with this, several NOEs are observed between the β- and γ-methylenes of Lys^{9} and the aromatic protons of Phe^{6}, which are absent in the minor isomer. The upfield shifting of methylenes in Lys^{9} as well as the observed NOEs involving Lys^{9} and Phe^{6} side chains are consistent with a cation-π stabilizing interaction between Lys^{9} and Phe^{6} [35].

The existence of peptide **1** as two conformational isomers resulting from the slow rotation through the amide bond in the betidamino acid 8 is hardly surprising. The ***Z***/***E*** isomerism is frequently common for *N*,*N*′-dialkylamides. However, the fact that the major conformational isomer corresponds to the ***Z*** isomer, having the most bulky groups – the naphthyl and the substituted Cα – in a *cis* orientation, is rather curious. This indicates that there must be some driving force for this conformational bias towards the *cis* orientation. We believe that probably the previously mentioned aromatic $\pi-\pi$ and cation–π interactions involving Phe^{6}, AGL^{8} and Lys^{9} play a major role in this conformational preference.

The question to answer is which one of the two conformational isomers is responsible for the biological activity. We hypothesize that it is the major isomer of peptide **1** that interacts with the SSTR3 receptor. We could think that the presence of a monoalkylamide instead of an *N*,*N*′-dialkylamide in the side chain of residue 8 of peptide **1** would favour the existence of the ***E*** isomer as the only one or, at least, the major one. It would be interesting to know the effect in binding affinity of changing from a major ***Z*** isomer to a major ***E*** isomer. Actually, a close analogue to peptide **1** in which the N$^{\beta}$–methyl group of AGL^{8} has been suppressed (analogue **5**, Table 1, Ref. 14) loses the binding affinity (IC_{50} > 1000 nM) for SSTR3. Although the 3D structure of this analogue is unknown, it seems reasonable to suppose a preference for the ***E*** isomer. This supports the idea that the N$^{\beta}$–methyl group takes a key role favouring the ***Z*** isomer of peptide **1**. The proximity and spatial orientation of Phe^{6}, AGL^{8} and Lys^{9} in this isomer suggests that this triplet of residues could be crucial for binding affinity and selectivity of peptide **1** for SSTR3 receptor.

The 3D structure of our SSTR3-selective somatostatin analogue (peptide **1**) can be compared with the consensus structural motifs of somatostatin analogues binding predominantly to SSTR1 [10], SSTR2/SSTR5 [11,12] and SSTR4 [13] receptors. We focus the comparison on the major conformational isomer of peptide **1** only.

The structural motif of the proposed pharmacophore for SSTR2/SSTR5-selective analogues involves a unique set of Cγ distances between the side-chains of D-Trp^{8}, Lys^{9} and Phe^{7}. The Cγ–Cγ distances between residues Tyr^{7}-AGL^{8} and Tyr^{7}-Lys^{9} in the conformers representing the 3D structure of peptide **1** are compatible with those between equivalent residues in the consensus structure of the SSTR2/SSTR5-selective analogues (Table 4). However, the naphthyl/indole (residue 8) is further away from the amino-alkyl of Lys^{9} in the structure of **1** than in the structural motif for SSTR2/SSTR5-selective analogues. The presence of the N$^{\beta}$–methyl amide in the side chain of AGL^{8} extends the conformational space occupied by this residue as compared to that of Trp^{8} and moves the naphthyl away from the Lys^{9} side chain. This difference could explain the low binding affinity (IC_{50} > 10 000 nM) of peptide **1** for SSTR2/SSTR5 receptors.

The proposed pharmacophore for SSTR1-selective analogues requires a unique arrangement of the side chains of Phe^{6}/Phe^{7}, D-Trp^{8}, IAmp^{9} and Phe^{11}, which is important for selective binding. When comparing the Cγ–Cγ distances involving these amino acids to those between the Cγ of equivalent residues – Phe^{6}/Tyr^{7}, AGL^{8}, Lys^{9} and Phe^{11} – of peptide **1** (Table 4), a

Table 4 Cγ–Cγ distances (Å) between residues involved in the proposed pharmacophores for SSTR1, SSTR2/SSTR5 and SSTR4 selective analogues. Cγ–Cγ distances between equivalent residues are shown for peptides **1** and **2**

	Ar^6–Ar^8	Ar^6–Lys^9	Ar^8–Lys^9	Ar^7–Lys^9	Ar^7–Ar^8	Lys^9–Phe^{11}	Ar^8–Phe^{11}	Ar^6–Phe^{11}
Peptide **1**[a] (major isomer) (SSTR3-selective analogue)	6.3 ± 0.1	6.2 ± 0.6	6.4 ± 0.2	9.5 ± 0.3	7.0 ± 0.6	6.4 ± 0.7	12.1 ± 0.6	11.1 ± 0.6
Pharmacophore [10] SSTR1-selective analogues	6–7.5	9–11	7–8	9–11	6–7.5	8–10	9.5–12	—
Pharmacophore [11,12] SSTR2/SSTR5-selective analogues	11–15	12–15	4	9–11	7–9	—	—	—
Pharmacophore [13] SSTR4-selective analogues	5.5–9.5	4.5–6.5	4.05–6.5	—	—	4.5–6.5	5.5–9.5	—
Peptide **2**[a] (non-selective)	7.8 ± 0.7	7.8 ± 0.7	4.8 ± 0.8	9.1 ± 0.6	6.6 ± 0.4	10.2 ± 0.9	12.4 ± 0.9	9.1 ± 1.5

[a] Average distance and standard deviation calculated from the ensemble of ten structures.

significant difference is observed for distances involving Phe^6-Lys^9 and also for Phe^{11}-Lys^9. These observations agree with the low binding affinity of peptide **1** for SSTR1 receptors.

Finally, the proposed pharmacophore for SSTR4-selective analogues involves a unique arrangement of the indole at aromatic residue 8 (Ar^8), the amino-alkyl of Lys^9 and an aromatic ring at position 6 or 11. The comparison of the triplet of residues Ar^8, Lys^9 and Phe^6 in this pharmacophore with the spatial orientation of AGL^8, Lys^9 and Phe^6 residues in peptide **1** – our SSTR3-selective analogue – shows a close similarity, as can be derived from the comparison of the Cγ–Cγ distances between side chains of the involved residues (Table 4). The distance between the C2 of residue AGL^8 and Cγ of Phe^6 (6.3 ± 0.1 Å) in **1** is within the distance range (5.5–9.5 Å) found in the SSTR4 pharmacophore model between the Cγ of Ar^8 (residue 8 is either Trp or D-Trp in the most SSTR4-selective analogues (Ref. 13)) and Phe^6; Ar^8 and Lys^9 are also in close proximity both in peptide **1** (6.4 ± 0.2 Å) and in the pharmacophore (4.5–6.5 Å), and the same happens to Phe^6 and Lys^9, with Cγ distances of 6.2 ± 0.6 Å in peptide **1** and 4.5–6.5 Å in the consensus structural motif of SSTR4-selective SRIF analogues. On the other hand, the spatial arrangement of the triplet constituted by residues 8, Lys^9 and Phe^{11} in peptide **1** does not fulfil the requirements of the pharmacophore proposed for SSTR4-selective analogues, mainly because the Cγ of Phe^{11} is more than 12 Å far from the C2 of AGL^8 (Table 4). This fact could explain the low binding affinity (IC_{50} > 1000 nM) of peptide **1** for SSTR4-receptors. Considering the previous observations, the pharmacophore for SSTR3-selective analogues could involve the side chains of Phe^6, AGL^8 and Lys^9, but would require the presence of a fourth residue. Additional studies are being carried out to further validate this hypothesis (Grace, C. R. R., Erchegyi, J., Reubi, J. C., Rivier, J., Riek, R., in preparation).

In order to get a deeper comprehension, from a structural point of view, of the selectivity of peptide **1** for SSTR3 receptors, we decided to determine the 3D structure of a non-selective SRIF analogue, des-$AA^{1,2,4,5,12,13}$-[Tyr^7, D-$2Nal^8$]-SRIF (peptide **2**). This peptide binds non-selectively to all of the receptors except SSTR1. It differs from peptide **1** only by D-$2Nal^8$.

The 3D structure of peptide **2** (Figure 5) shows a turn-like structure around D-$2Nal^8$-Lys^9, supported by sequential and medium-range backbone NOEs $d_{\alpha N(i,i+2)}$ (Figure 3(C)). The relatively low temperature coefficient of −3.2 ppb/K observed for the amide hydrogen of Thr^{10} suggests a hydrogen-bonded and exchange-protected NH. However, the carbonyl C=O of Tyr^7 is not in a hydrogen-bond favourable orientation with respect to the NH of Thr^{10}. On the basis of the backbone torsion angles (Table 3), although the Φ and Ψ values of D-$2Nal^8$ are compatible with a β-turn of type II', the Φ angle of Lys^9 is far from the expected value (−80) for this type of β-turn. The side chain of D-$2Nal^8$ is in the *trans* rotamer and that of Lys^9 is in the *gauche*$^-$ rotamer. As a consequence, the side chains of these two residues are close to each other in space, pointing away from the backbone plane. The proximity of these residues is supported by the characteristic and significant upfield shift of the Lys^9 side-chain protons, γH and δH specially, caused by the ring current of the naphthyl ring, and by an NOE between the aromatic H4 of D-$2Nal^8$ and the εH of Lys^9. Both Phe^6 and Tyr^7 aromatic rings are in the *trans* rotamers, and they orient perpendicularly to the backbone plane in divergent directions.

When comparing the 3D structures of peptides **1** (major conformational isomer) and **2**, several differences are observed. Considering that the aromatic residue in position 8 and Lys^9 are involved in the essential pharmacophore of somatostatin, it is interesting to compare the mean 3D structures of both analogues by

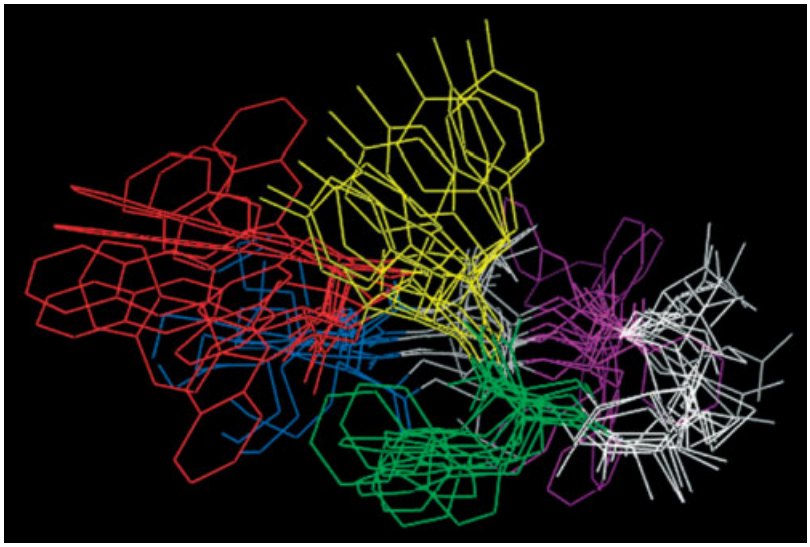

Figure 5 Bundle of ten conformers representing the 3D structure of peptide **2**.

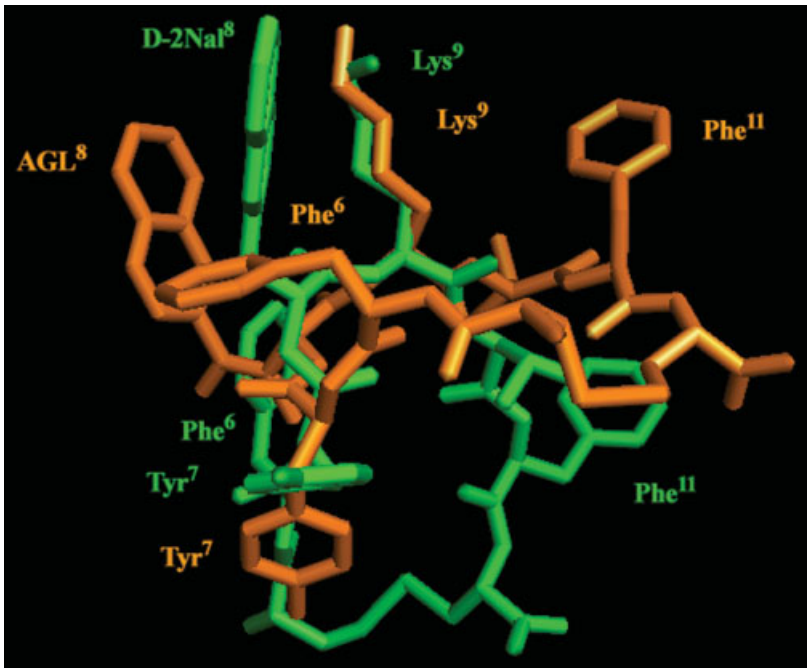

Figure 6 Comparison of the average 3D structures of peptides **1** (orange) and **2** (green).

superimposing these residues. Because of the different side-chain length of residue 8 in the two analogues, only Lys^9 residues in the average structures of **1** and **2** have been superimposed (*rmsd* = 2 Å for all atoms of this residue). This comparison shows that the backbone planes defined by the macrocycle of each analogue are perpendicular (Figure 6). The backbone of peptide **2** (green colour) stays along the plane of the Figure, with the side chains of D-2Nal^8 and Lys^9 pointing upwards in the same plane. On the other hand, the backbone of **1** (orange colour) remains in a perpendicular plane, where the Cα of AGL^8, Lys^9 and Phe^{11} stay at the back and the Cα of Phe^6 and the S–S bridge are in front, facing the reader. When comparing the spatial orientation of equivalent side chains, it is clear that the aromatic rings of Tyr^7 explore a very similar conformational space in both analogues. The naphthyl group of residue 8 also has a similar orientation. However, the side chains of Phe^6 and Phe^{11} explore completely different conformational regions. While both side chains are surrounding the amino-alkyl of Lys^9 in peptide **1**, staying relatively close to each other, both side chains of Phe^6 and Phe^{11} remain rather far from Lys^9 in peptide **2** (see Cγ–Cγ distances, Table 4).

Assuming that the intrinsic orientation of the side chains might be prearranged when the analogues

bind to receptors, we propose that both Phe[6] and Phe[11] have a key role in determining selectivity of peptide **1** for SSTR3 receptors and that the relative spatial orientation of Phe[6], AGL[8], Lys[9] and Phe[11] in peptide **1** could be a pharmacophore of SSTR3-selective analogues. Additional structural studies of other SSTR3-selective and non-selective analogues are being carried out to confirm the proposed pharmacophore model for these receptors (Grace, C. R. R., Erchegyi, J., Reubi, J. C., Rivier, J., Riek, R., in preparation).

CONCLUSIONS

The 3D conformations of two potent SRIF analogues, one selective for SSTR3 receptors (peptide **1**) and the other non-selective (peptide **2**) have been studied in water. Two independent structures have been determined for the two conformational isomers of analogue **1**, caused by the presence of the betidamino acid AGL[8]. The major isomer corresponds to the ***Z*** isomer and the minor one to the ***E*** isomer. The 3D structure of the major conformational isomer has been compared to the proposed pharmacophores for SSTR1, SSTR2/SSTR5 and SSTR4-selective analogues. While significant differences have been observed between the structure of **1** and the pharmacophores of SSTR1- and SSTR2/SSTR5-selective analogues, the relative spatial orientation of the side chains defining the consensus structure of SSTR4-selective analogues is partially satisfied in analogue **1**. On the basis of the comparison of the 3D structures of peptides **1** and **2**, and considering the previously mentioned pharmacophores, a structural motif has been proposed that could be responsible for SSTR3 selectivity. This is constituted by the side chains of a central Lys[9], surrounded by the side chains of three aromatic residues, Phe[6], AGL[8] and Phe[11].

Acknowledgements

The reported studies were partially supported by Grant DK059953 from the National Institutes of Health. We acknowledge the NMR Facility of Serveis Cientificotècnics at Universitat de Barcelona for allocating time to carry out the NMR experiments. We thank Debbie Doan for manuscript preparation.

REFERENCES

1. Brazeau P, Vale WW, Burgus R, Ling N, Butcher M, Rivier JE, Guillemin R. Hypothalamic polypeptide that inhibits the secretion of immunoreactive pituitary growth hormone. *Science* 1973; **179**: 77–79.
2. Epelbaum J. Somatostatin in the central nervous system: physiology and pathological modifications. *Prog. Neurobiol.* 1986; **27**: 63–100.
3. Guillemin R, Gerich JE. Somatostatin: physiological and clinical significance. *Annu. Rev. Med.* 1976; **27**: 379–388.
4. Patel YC. Somatostatin and its receptor family. *Front. Neuroendocrinol.* 1999; **20**: 157–198.
5. Olias G, Viollet C, Kusserow H, Epelbaum J, Myerhof W. Regulation and function of somatostatin receptors. *J. Neurochem.* 2004; **89**: 1057–1091.
6. Reisine T, Bell GJ. Molecular biology of somatostatin receptors. *Endocrinol. Rev.* 1995; **16**: 427–442.
7. Lamberts S, Krenning E, Reubi JC. The role of SRIF and its analogs in the diagnosis and treatment of tumors. *Endocrinol. Rev.* 1991; **12**: 450–482.
8. Hofland LJ, Visser-Wisselaar HA, Lamberts SW. Somatostatin analogs: clinical application in relation to human somatostatin receptor subtypes. *Biochem. Pharmacol.* 1995; **50**: 287–297.
9. Janecka A, Zubrzycka M, Janecki T. Review. Somatostatin analogs. *J. Pept. Res.* 2001; **58**: 91–107.
10. Grace CRR, Durrer L, Koerber SC, Erchegyi J, Reubi JC, Rivier JE, Riek R. Somatostatin receptor 1 selective analogues: 4. Three-dimensional consensus structure by NMR. *J. Med. Chem.* 2005; **48**: 523–533, DOI: 10.1021/jm049518u.
11. Huang Z, He Y, Raynor K, Tallent M, Reisine T, Goodman M. Main chain and side chain chiral methylated somatostatin analogs: synthesis and conformational analyses. *J. Am. Chem. Soc.* 1992; **114**: 9390–9401.
12. Melacini G, Zhu Q, Osapay G, Goodman M. A refined model for the somatostatin pharmacophore: conformational analysis of lanthionine-sandostatin analogs. *J. Med. Chem.* 1997; **40**: 2252–2258.
13. Grace CRR, Koerber SC, Erchegyi J, Reubi JC, Rivier JE, Riek R. Novel sst4-selective somatostatin (SRIF) agonists. 4. Three-dimensional consensus structure by NMR. *J. Med. Chem.* 2003; **46**: 5606–5618, DOI: 10.1021/jm030246p.
14. Reubi JC, Schaer JC, Wenger S, Hoeger C, Erchegyi J, Waser B, Rivier JE. Sst3-selective potent peptidic somatostatin receptor antagonists. *Proc. Natl. Acad. Sci. U.S.A.* 2000; **97**: 13 973–13 978, DOI: 10.1073/pnas.250483897.
15. Jiang G, Miller C, Koerber SC, Porter J, Craig AG, Bhattacharjee S, Kraft P, Burris TP, Campen CA, Rivier CL, Rivier JE. Betidamino acids scan of the GnRH antagonist acyline. *J. Med. Chem.* 1997; **40**: 3739–3748.
16. Erchegyi J, Penke B, Simon L, Michaelson S, Wenger S, Waser B, Cescato R, Schaer J-C, Reubi JC, Rivier J. Novel sst_4-selective somatostatin (SRIF) agonists. Part II: Analogues with β-methyl-3-(2-naphthyl)-alanine substitutions at position 8. *J. Med. Chem.* 2003; **46**: 5587–5596.
17. Wüthrich K. *NMR of Proteins and Nucleic Acids*. John Wiley & Sons: New York, 1986.
18. Davis DG, Bax A. Assignment of complex ^{1}H NMR spectra via two-dimensional homonuclear Hartmann-Hahn spectroscopy. *J. Am. Chem. Soc.* 1985; **107**: 2820–2821.
19. Rance M, Sorensen OW, Bodenhausen B, Wagner G, Ernst RR. Improved spectral resolution in COSY 1H NMR spectra of proteins via double quantum filtering. *Biochem. Biophys. Res. Commun.* 1983; **117**: 479–485.
20. Macura S, Ernst RR. Elucidation of cross-relaxation in liquids by two-dimensional NMR spectroscopy. *Mol. Phys.* 1980; **41**: 95–117.
21. Bax A, Davis DG. Practical aspects of two-dimensional transverse NOE spectroscopy. *J. Magn. Reson.* 1985; **63**: 207–213.
22. Piotto M, Saudek V, Sklenar V. Gradient-tailored excitation for single-quantum NMR spectroscopy of aqueous solutions. *J. Biomol. NMR* 1992; **2**: 661–665.
23. Hwang TL, Shaka AJ. Water suppression that works. Excitation sculpting using arbitrary waveforms and pulsed field gradients. *J. Magn. Reson., A* 1995; **112**: 275–279.
24. Willker W, Leibfritz D, Kerssebaum R, Lohman J. Gradient-selected E.COSY. *J. Magn. Reson., A* 1993; **102**: 348–350.

25. Hyberts SG, Märki W, Wagner G. Stereospecific assignments of side chain protons and characterization of torsion angles in Eglin c. *Eur. J. Biochem.* 1987; **164**: 625–635.
26. Delaglio F, Grzesiek S, Vuister GW, Zhu G, Pfeifer J, Bax A. NMRPipe: a multidimensional spectral processing system based on UNIX pipes. *J. Biomol. NMR* 1995; **6**: 277–293.
27. Johnson BA, Blevins RA. NMRView: a computer program for the visualization and analysis of NMR data. *J. Biomol. NMR* 1994; **4**: 603–614.
28. Brunger AT, Adams PD, Clore GM, DeLano WL, Gros P, Grosse-Kunstleve RW, Jiang J-S, Kuszewski J, Nilges M, Pannu NS, Read RJ, Rice LM, Simonson T, Warren GL. Crystallography & NMR system: a new software suite for macromolecular structure determination. *Acta Crystallogr., D* 1998; **54**: 905–921.
29. Kleywegt GJ, Jones TA. Databases in protein crystallography. *Acta Cryst.* 1998; **D54**: 1119–1131 (CCP4 Proceedings) http://xray.bmc.uu.se/hicup/, [last accessed November 2005].
30. Humphrey W, Dalke A, Schulten K. VMD-Visual molecular dynamics. *J. Mol. Graphics* 1996; **14**: 33–38.
31. DeLano Scientific LLC. http://www.pymol.sourceforge.net, [last accessed November 2005].
32. Rose GD, Gierasch LM, Smith JA. Turns in peptides and proteins. *Adv. Protein Chem.* 1985; **37**: 1–109.
33. Andersen NH, Neidigh JW, Harris SM, Lee GM, Liu Z, Tong H. Extracting information from the temperature gradients of polypeptide NH chemical shifts. 1. The importance of conformational averaging. *J. Am. Chem. Soc.* 1997; **119**: 8547–8561.
34. Markley JL, Bax A, Arata Y, Hilbers CW, Kaptein R, Sykes BD, Wright PE, Wüthrich K. Recommendations for the presentation of NMR structures of proteins and nucleic acids. *J. Mol. Biol.* 1998; **280**: 933–952.
35. Waters ML. Aromatic interactions in peptides: impact on structure and function. *Biopolymers* 2004; **76**: 435–445.